Case Studies in Thermal Engineering 5 (2015) 13–23

Contents lists available at ScienceDirect

Case Studies in Thermal Engineering

journal homepage: www.elsevier.com/locate/csite

Enhance heat transfer in the channel with V-shaped wavy lower plate using liquid nanofluids

Azher M. Abed [a,b,*], K. Sopian [a], H.A. Mohammed [c], M.A. Alghoul [a], Mohd Hafidz Ruslan [a], Sohif Mat [a], Ali Najah Al-Shamani [a]

[a] Solar Energy Research Institute (SERI), Universiti Kebangsaan Malaysia, 43600 Bangi, Selangor, Malaysia
[b] Department of Air conditioning and Refrigeration, Al-Mustaqbal University College, Babylon, Iraq
[c] Departments of Thermofluids, Faculty of Mechanical Engineering, Universiti Teknologi Malaysia, 81310 UTM Skudai, Johor Bahru, Malaysia

ARTICLE INFO

Article history:
Received 13 September 2014
Received in revised form
22 October 2014
Accepted 2 November 2014
Available online 11 November 2014

Keywords:
Heat transfer enhancement
Nanofluids
Corrugated channels
Turbulent flow

ABSTRACT

The heat transfer and flow characteristics in corrugated with V-shape lower plate using nanofluids are numerically studied. The computations are performed on uniform heat flux over a range of Reynolds number (Re) 8000–20,000. The governing equations are numerically solved in the domain by a finite volume method (FVM) using the k–ε standard turbulent model. Studies are carried out for different types of nanoparticles Al_2O_3,CuO, SiO_2 and ZnO with different volume fractions in the range of 0–4%. Three different types of base fluid (water, glycerin, ethylene glycol) are also examined. Results indicated that the average Nusselt number for nanofluids is greater than that of the base liquid. The SiO_2 nanofluid yields the best heat transfer enhancement among all other type of nanofluids. Heat transfer enhancement increase with increases the volumetric concentration, but it is accompanied by increasing pressure drop values. Moreover, the average Nusselt number increases with an increase in Reynolds number and volume concentration. The SiO_2–glycerin nanofluid has the highest Nusselt number compared with other base fluids. The present study shows that these V-shaped wavy channels have advantages by using nanofluids and thus serve as promising candidates for incorporation into efficient heat transfer devices.

1. Introduction

In the development of energy-efficient heat transfer fluids, the thermal conductivity of the heat transfer fluids plays a vital role. Despite considerable previous research and development efforts on heat transfer enhancement, major improvements in cooling capabilities have been constrained because traditional heat transfer fluids used in today's thermal management systems, such as water, oils, and ethylene glycol, have inherently poor thermal conductivities, orders-of-magnitude smaller than those of most solids. Due to increasing global competition, a number of industries have a strong need to develop advanced heat transfer fluids with significantly higher thermal conductivities than are presently available. Corrugated surface geometry is one of the many suitable passive techniques to enhance the heat transfer in heat exchangers due to growing recirculation regions near the corrugated wall and hence, enhances the mixing of fluid as well as heat transfer. On the coolant side, the use of nanofluids, a liquid in which nanoparticles are added to a base fluid, can also enhance the heat transfer due to the improved thermal conductivity of the fluid. Several investigators have investigated of conventional fluid through corrugated channel numerically and experimentally. In the

* Corresponding author at: Solar Energy Research Institute (SERI), Universiti Kebangsaan Malaysia, 43600 Bangi, Selangor Malaysia.
E-mail address: azhermuhson@gmail.com (A.M. Abed).

http://dx.doi.org/10.1016/j.csite.2014.11.001
2214-157X/

Nomenclature

A	area (m^2)
Al_2O_3	aluminum oxide
Cu	copper
CuO	copper oxide
CPHE	corrugated plate heat exchanger
C_ε	turbulent model constant
C_μ	turbulent model constant
C_P	specific heat (kJ/kg K)
C_f	skin-friction coefficient
CFD	computational fluid dynamic
D_h	hydraulic diameter (mm); $D_h = H_{max} + H_{min}$
d_p	diameter of nanofluid particles
d_f	equivalent diameter of a base fluid molecule
E	enhancement ratio
E	total energy (J), (KJ), (cal.), (Btu)
EG	ethylene glycol
f	friction factor, $f = 2\ \Delta p(D_h/L)(1/\rho u^2)$
Fe	Iron
FVM	finite volume method
h	heat transfer coefficient (W/m^2 K)
H	half distance of the channel height (mm)
H_{min}	height of the bottom channel (mm)
H_{max}	height of the top channel (mm)
H_w	height of wavy (mm)
H_2O	Water
I	turbulent intensity
k	thermal conductivity of the fluid (W/m K)
k	turbulent kinetic energy
L	turbulence characteristics length = 0.07(Dh/2)
M	molecular weight of base fluid
N	Avogadro number $= 6.022 \times 10^{-23}$ mol^{-1}
Nu	Nusselt number
ΔP	pressure drop (kPa)
p	wet perimeter (m)
PHE	plate heat exchanger
Pr	Prandtl number, $Pr = C_p\mu/k$
Q	heat transfer rate (kW)
q	heat flux (W/m^2)
Re	Reynolds number ($Re = \rho\, u_{i\ D_h}/\mu$)
RSM	Reynolds stress model
SiO_2	silicon dioxide
SKE	standard k–ε model
T	temperature (K)
T_0	reference temperature (293 K)
u	velocity component at x-direction
U	mean velocity distribution at x-direction
u'	velocity fluctuation
X	distance along the x-co-ordinate
ZnO	zinc oxide

Greek symbols

β	fraction of liquid volume traveling with a particle
μ	dynamic viscosity of the fluid (pas)
ρ	density (kg/m^3)
θ	wavy angle
$\tilde{\sigma}$	length of corrugated (mm)
$\overline{X}$	length of domain (mm)
$\varnothing$	volume fraction (%)
ϕ	scalar variable
ε	dissipation kinetic energy (m^2/s^3)
σ_k	diffusion Prandtl number for k
τ_s	wall shear stress
κ	Boltzmann constant (1.3807×10^{-2} J/K)

Subscripts

cr	cross section
corr	corrugated channel
s	start point of corrugated wall
stra	straight channel
in	inlet
ave	average
out	outlet
e	end point of corrugated wall
eff	effective
f	base fluid
nf	nanofluid
min	minimum
max	maximum
m	mean
p	particles
w	wall
x	local value
b	bulk

literature [1–5] it is shown that the use of a corrugated channel results in a more complex flow structure and improves the heat transfer by as much as two or three times compared to a conventional straight channel. Naphon and Kornkumjayrit [6–8] conducted numerical and experimental study forced convection of the heat transfer and flow developments in the channel with V-corrugated upper and lower plates which all configuration peaks lie in an in phase arrangement The corrugated plates with three different corrugated tile angles of 20°, 40°, and 60° were tested with the height of the channel of 12.5 mm. It can be found that the corrugated surface has significant effect on the enhancement of heat transfer and pressure drop. Numerous experimental and numerical studies have been performed on heat transfer enhancement by improving thermal conductivity using nanofluids and varied methods. Lee et al. [9] measured the thermal conductivity of (EG) based nanofluid containing ZnO. Thermal conductivity enhancement of an EG-based ZnO nanofluid was successfully achieved using the one-step PWE method. Das et al. [10] presented investigations on the increase of thermal conductivity with temperature of Al_2O_3 and CuO water-based nanofluids. The values of particle diameters was 38.4 nm for Al_2O_3 while 28.6 nm for CuO. Nanofluids containing smaller particles (CuO) showed greater enhancements of thermal conductivity with temperature than larger particles. Recently, Vajjha and Das [11,12] investigated

experimentally the relative effects of three nanofluids containing, Al_2O_3,CuO, SiO_2 and ZnO nanoparticles. Particle volumetric concentration tested was up to 10% and the temperature range of the experiments was from 298 to 363 K. Based on their experimental data extended the Koo and Kleinstreuer [13] model for Ethylene Glycol–Water (EG/W) has been as base fluid. Corcione [14] developed two empirical equations for the evaluation of the nanofluid effective thermal conductivity and dynamic viscosity. The heat transfer enhancement deriving from the dispersion of solid nanoparticles into a base liquid has been calculated for different values of the average temperature of the nanofluid in the range between 294 K and 324 K, the nanoparticle diameter in the range between 25 nm and 150 nm, as well as for three different nanoparticle materials (i.e., Cu, Al_2O_3, and TiO_2) and two different base fluids (i.e., water and ethylene glycol). Heidary and Kermani [15] studied numerically the effects of nanofluids on the heat transfer and flow field in a wavy channel. Copper–water nano-fluid is considered for simulation. Results show that the addition of nano-particles to the pure fluid and construction of wavy walls can significantly enhance the heat exchange between the wall and the flow. It is observed that the addition of 10% nano-particles can enhance the heat exchange by 25%.

Ahmed et al. [16,17] studied numerically forced convection of flow and heat transfer enhancement in a corrugated channel using CuO nanofluid. The results show that the heat transfer increases as the volume fraction of nanoparticle increases. In addition, as the volume fraction increases, the pressure drop slightly increases for all value of Reynolds number. For same value of volume fraction, the heat transfer enhancement was found to depend on Reynolds number.

There are two different approaches to investigate the heat transfer enhancement of the suspensions: the two-phase one and the single-phase one. The first provides the possibility of understanding the functions of both the fluid phase and the solid particle in the heat transfer process, but needs much computation time and computer capacity. The second assumes that both the fluid phase and particles are in a thermal equilibrium state and they flow at the same velocity. This approach is simpler and takes less computation time. In cases that the main interest is focused on heat transfer process, this approach may be more suitable [18].

Xuan and Roetzel [19] analyzed the heat transfer mechanism in nanofluids based on single phase and two-phase flow approaches. In this study, it was considered that the nanofluids to behave like a fluid and used for the purpose of heat transfer enhancement. Since the solid particles are ultrafine (<100 nm) and they are easily fluidized. Under the assumptions that there exist no motion slip between the discontinuous phase of the dispersed ultrafine particles and the continuous liquid and the local thermal equilibrium between the nanoparticles and the fluid, the nanofluid can be treated as the common pure fluid. All the equations of continuity, motion, and energy for the pure fluid are directly extended to the nanofluid. Buongiorno and Jacopo [20] considered seven slip mechanisms that can produce a relative velocity between the nanoparticles and the base fluid. These are inertia, Brownian diffusion, thermophoresis, diffusiophoresis, Magnus effect, fluid drainage, and gravity. It was concluded that, of these seven, only Brownian diffusion and thermophoresis are important slip mechanisms in nanofluids. Furthermore, a comparison of the nanoparticle and turbulent eddy time and length scales clearly indicates that the nanoparticles move homogeneously with the fluid in the presence of turbulent eddies, so an effect on turbulence intensity is also doubtful. Bianco et al. [21] investigated the laminar forced convection flow of a nanofluid in a circular tube based on single phase and two-phase flow approaches. It was demonstrated that the maximum difference in the average heat transfer coefficient between single- and two-phase models results is about 11%.

The above survey; the numerous experimental and theoretical studies have been reported concerning the heat transfer enhancement using nanofluid in the corrugated PHE. However, no data reported on thermal and flow field in the corrugated channel with V-shape corrugated lower plate using nanofluid.

The present study examines 2D turbulent flow convective heat transfer and flow characteristics in corrugated with V-shape lower plate with uniform heat flux by using different types of nanofluids, different nanoparticle volume fractions, are dispersed in different base fluids (water, glycerin, and ethylene glycol). This investigation covers Reynolds number in the range of 8000–20,000, different types of nanofluids and different volume fractions ranged from 0% to 4%.

Results of interests such as Average Nusselt number, pressure drop, Average Nusselt Number Enhancement, in corrugated channel with V- shape corrugated lower plate are reported to illustrate the effect of nanofluids on these parameters.

2. Mathematical modeling

2.1. Physical model and assumptions

The schematic diagram of the investigation domain is shown in Fig. 1(a) which consisted of a lower corrugated plate and upper flat wall. The corrugated channels with corrugated tilt angle of 60° are tested with the height of the channel of 17.5 mm and height of the wavy of 2.5 mm.The length of each adiabatic flat section before, and after the corrugated section is 100–200 mm.

2.2. Governing equations

By considering the geometry and physical problem as shown in Fig. 1, the k–ε standard turbulence model [22] is used to simulate the turbulent heat transfer and flow characteristics. The main governing equations [22] can be written in the following form:

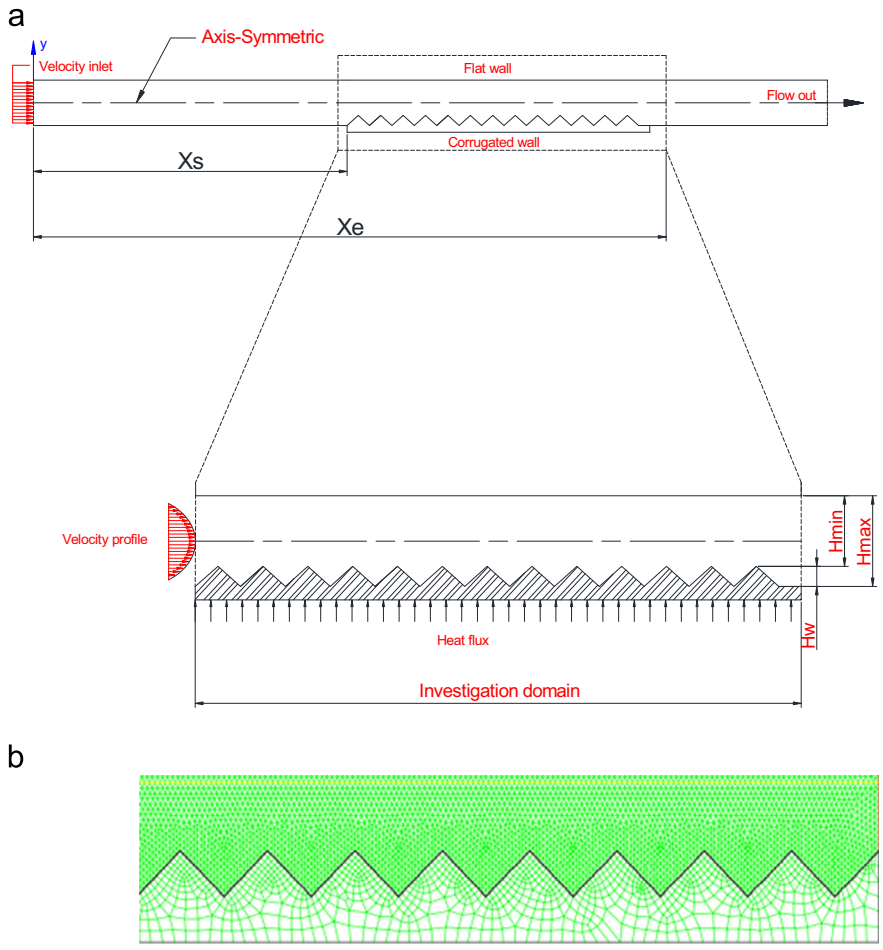

Fig. 1. Schematic diagram of the V-shaped wavy lower plate: (a) investigation domain, and (b) Mesh generation.

Continuity equation

$$\frac{\partial}{\partial x_i}(\rho u_i) = 0 \tag{1}$$

where the symbol ρ is the density of fluid and u_i is the axial velocity.

The momentum conservation equation is

$$\frac{\partial}{\partial x_j}(\rho\, u_i u_j) = -\frac{\partial p}{\partial x_i} + \frac{\partial}{\partial x_j}\left[\mu\left(\frac{\partial u_i}{\partial x_j} + \frac{\partial u_j}{\partial x_i} - \frac{2}{3}\delta_{ij}\frac{\partial u_i}{\partial x_j}\right)\right] + \frac{\partial}{\partial x_j}\left(-\rho\overline{u_i' u_j'}\right) \tag{2}$$

The energy equation is

$$\frac{\partial}{\partial x_i}[u_i(\rho E + p)] = \frac{\partial}{\partial x_j}\left[\left(k + \frac{c_p \mu_t}{Pr_t}\right)\frac{\partial T}{\partial x_j} + u_i(\tau_{ij})_{eff}\right] \tag{3}$$

The symbols μ, u' and u_j, are the fluid viscosity, fluctuated velocity and the velocity in y-direction respectively, the term $\rho\overline{u_i' u_j'}$ is the turbulent shear stress.

In the present numerical study, k–ε turbulent model proposed by Launder and Spalding [23] was employed to express the turbulent stresses and heat flux quantities of the related physical phenomenon. k–ε turbulent model introduces two additional equations. These equations are turbulent kinetic energy (k) and rate of dissipation (ε). The equations for turbulent kinetic energy (k) and rate of dissipation (ε) are given by

Turbulent kinetic energy (k) equation

$$\frac{\partial}{\partial x_i}(\rho k u_i) = \frac{\partial}{\partial x_j}\left[\left(\mu + \frac{\mu_t}{\sigma_k}\right)\frac{\partial k}{\partial x_j}\right] + G_k - \rho\varepsilon \tag{4}$$

Turbulent kinetic energy dissipation (ε) equation

$$\frac{\partial}{\partial x_i}(\rho\varepsilon u_i)=\frac{\partial}{\partial x_j}\left[\left(\mu+\frac{\mu_t}{\sigma_\varepsilon}\right)\frac{\partial e}{\partial x_j}\right]+C_{1\varepsilon}(\varepsilon/k)G_k+C_{2\varepsilon}\rho(\varepsilon^2/k) \tag{5}$$

In the above equations, G_k represents the generation of turbulent kinetic energy due to mean velocity gradients, σ_k and σ_ε are effective Prandtl numbers for turbulent kinetic energy and rate of dissipation, respectively; $C_{1\varepsilon}$ and $C_{2\varepsilon}$ are constants and μ_t is the eddy viscosity and is modeled as

$$\mu_t=(\rho C_\mu k^2)/\varepsilon \tag{5.1}$$

The empirical constants for the turbulence model are arrived by comprehensive data fitting for a wide range of turbulent flow [22]

$$C_\mu=0.09,\ C_{\varepsilon1}=1.47,\ C_{\varepsilon2}=1.92,\ \sigma_k=1.0,\ \sigma_\varepsilon=1.3 \tag{5.2}$$

Given the complexity of these equations, computational methods of solving them are required.

2.3. Boundary conditions

In the present study, the boundary conditions imposed at the upper and lower corrugated walls are no slip and constant heat flux, while the flat walls are thermally insulated. The flow is assumed Newtonian, turbulent, two-dimensional and incompressible. As the flow is much higher, the buoyancy effect has been neglected. Velocity boundary condition is applied at the inlet while the pressure boundary condition is used at the outlet [4]. The boundary conditions for a steady, two-dimensional flow rate are as follows:

At the wall

$$u=0,\ \ v=0,\ \ q=q_{wall} \tag{6}$$

where, u and v are the velocities.

Initial conditions

At the inlet, the uniform profiles for all the properties are as follows:

$$u=u_{in},\ \ v=0,\ \ T=T_{in}\ ,\ \ k=k_{in}\ ,\ \ \varepsilon=\varepsilon_{in} \tag{7}$$

At the outlet, the flow may safely be assumed as fully developed, which implies negligible stream wise gradients of all variables.

$$\frac{\partial\varnothing}{\partial n}=0;\quad \varnothing=u,\ v,\ p,\ k,\ \varepsilon,\ \omega \tag{8}$$

The turbulent kinetic energy, k_{in} and the turbulent dissipation ε_{in}, at the inlet section are approximated from the turbulent intensity, I [22]. The turbulent characteristics length, L, is follows:

$$k_{in}=\frac{3}{2}(u_{in}I)^2,\quad \varepsilon_{in}=C_\mu^{3/4}\frac{k^{3/2}}{L} \tag{9}$$

In the present study, the turbulence characteristics length, L is set to be 0.07 ($D_h/2$). The factor of 0.07 is based on the maximum value of the mixing length in the fully developed turbulent flow [22]. The turbulent intensity level, I, is defined the ratio of the root-mean-square of the velocity fluctuation, u', to the mean flow velocity, u, as follows:

$$I=\frac{u'}{u}\times 100\% \tag{10}$$

To represent the results and characterize the heat transfer and flow in the V-shaped corrugated channel, the following variable and parameters are presented.

The average heat transfer coefficient along the corrugated channel h_c, can be calculated from the average heat transfer rate obtained from [4]:

$$Q_{ave}=h_cA_c(\Delta T) \tag{11}$$

where A_c is the surface area of the corrugated plate.

The average heat transfer coefficient is presented in terms of average Nusselt number [4] as follows:

$$Nu=\frac{h_cH\tilde{\sigma}}{k\overline{X}} \tag{12}$$

where H is the half distance of the channel height, k is the thermal conductivity of fluid, $\overline{X}=(x_e-x_s)$ is the distance from the leading edge of the corrugated plate to the end of the domain, and $\tilde{\sigma}$ is the distance from the leading edge of the corrugated plate along the corrugated surface as shown in Fig. 1(a).

The local heat transfer $h(x)$ is defined as [24]

$$h(x)=q/T_s(x)-T_b(x) \tag{13}$$

q represents the heat flux, $T_s(x)$ and $T_b(x)$ are the local surface wall and bulk temperatures, respectively.

At the corrugated channel section, the inlet water temperature was taken as 300 K and the inlet water velocity was calculated using the following equation:

$$u_{in}=\frac{R_e\,\mu}{\rho D_h} \tag{14}$$

The hydraulic diameter is computed as [17, 24]

$$D_h=\frac{4A}{P}=H_{min}+H_{max} \tag{15}$$

where H_{min} and H_{max} are the height of the top and bottom channel as shown in Fig. 1.

The average value of friction coefficient for corrugated channel is [24]

$$C_{f,ave} = \frac{1}{x_e - x_s}\int_{x_s}^{x_e} C_{fx}\, dx \tag{16}$$

Since the friction factor is defined as

$$f = 4C_{fx} \tag{17}$$

The Fanning friction factor is defined as follows:

$$C_{fx} = 2\tau_s/\rho u_{in}{}^2 \tag{18}$$

τ_s is wall shear stress.

The pressure drop for the flow in the corrugated channel is computed as [24]

$$\Delta p = f\frac{(x_e - x_s)\rho u_{in}{}^2}{2D_h} \tag{19}$$

The effective density and heat capacity of the nanofluid at the reference temperature (T_0) is determined from the following equations [14]:

$$\rho_{nf} = (1-\phi)\rho_f + \phi\rho_p \tag{20}$$

where ρ_f and ρ_{nf} are the mass densities of the based fluid and the solid nanoparticles, respectively.

$$(\rho C_p)_{nf} = (1-\phi)(\rho C_p)_f + \phi(\rho\, C_p)_p \tag{21}$$

where $(\rho\, C_p)_f$ and $(\rho\, C_p)_p$ are heat capacities of the based fluid and the solid nanoparticles, respectively.

By using Brownian motion of nanoparticles in corrugated channel, the effective thermal conductivity can be obtained by using the following mean empirical correlation [11,12]

$$k_{eff} = k_{static} + k_{Brownian} \tag{22}$$

$$k_{static} = k_f\left[\frac{(k_p+2k_f) - 2\phi(k_f - k_p)}{(k_p+2k_f) + \phi\,(k_f - k_p)}\right] \tag{22.1}$$

$$k_{Brownian} = 5\times 10^4\, \beta\phi\rho_f\, C_{p,f}\sqrt{\frac{\kappa T}{2\rho_p d_p}} f(T,\ \phi) \tag{22.2}$$

where

Boltzmann constant: $\kappa = 1.3807 \times 10^{-23}$ J/K

Modeling, $f(T,\phi)$

$$f(T,\phi) = \left(2.8217\times 10^{-2}\phi + 3.917\times 10^{-3}\right)\left(\frac{T}{T_0}\right) + \left(-3.0669\times 10^{-2}\phi - 3.391123\times 10^{-3}\right) \tag{23}$$

For $1\% \le \phi \le 4\%$ and $300\ \text{K} < T < 325$ K.

The effective viscosity can be obtained by using the following mean empirical correlation [14]:

$$\mu_{eff} = \mu_f \frac{1}{(1 - 34.87\,(d_p/d_f)^{-0.3}\phi^{1.03})} \tag{24}$$

$$d_f = \left[\frac{6M}{N\pi\rho_f}\right]^{1/3} \tag{25}$$

Table 1
The values of β for different particles with its boundary conditions [11,12].

Type of particles	β	Concentration (%)	Temperature (K)
Al_2O_3	$8.4407(100\phi)^{-1.07304}$	$1\% \le \phi \le 10\%$	$298 \le T \le 363$
CuO	$9.881(100\phi)^{-0.9446}$	$1\% \le \phi \le 6\%$	$298 \le T \le 363$
SiO_2	$1.9526(100\phi)^{-1.4594}$	$1\% \le \phi \le 10\%$	$298 \le T \le 363$
ZnO	$8.4407(100\phi)^{-1.07304}$	$1\% \le \phi \le 7\%$	$298 \le T \le 363$

Table 2
The thermo physical properties of base fluid and nanoparticles at T=300 k.

Thermo-physical properties	Water	Glycerin	EG	Al_2O_3 [12]	CuO [12]	SiO_2 [12]	ZnO [11]
Density, ρ (kg/m^3)	996.5	1259.9	1114.4	3600	6500	2220	5600
Specific heat, C_p (J/kg K)	4181	2427	2415	765	533	745	495.2
Thermal conductivity, k (W/m K)	0.6103	0.286	0.252	36	17.65	1.4	13
Viscosity, μ (mpa s)	0.001003	0.799	0.0157	–	–	–	–

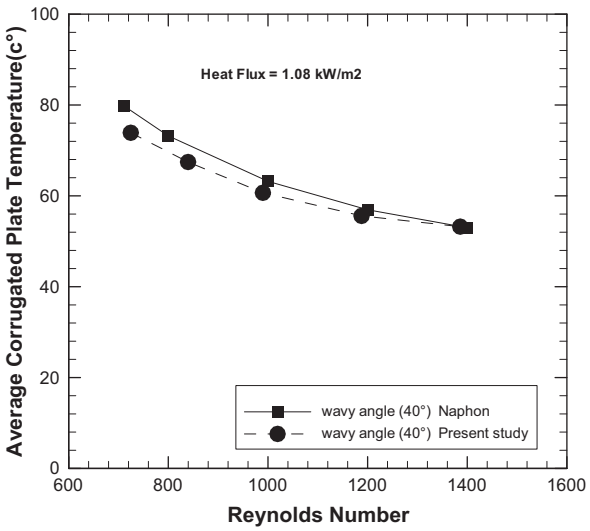

Fig. 2. Comparison of the average corrugated plate temperature of the present study with the results of Naphon [6] under the Reynolds number range.

where M is the molecular weight of base fluid, N is the Avogadro number $=6.022\times10^{23}$ mol^{-1} and ρ_f is the mass density of the based fluid calculated at temperature $T_0=293$ K (Table 2).

2.4. Numerical computation

Numerical analysis using commercial software (fluent 6.3) is performed in order to understand the flow characteristic in the corrugated channel. The governing Eqs. (1)–(5) are a set of convection equation with velocity and pressure coupling. It is based on the control volume method, SIMPLEC algorithm of Versteeg and Malalasekera [22] is used to deal with the problem of velocity and pressure coupling. Second-order upwind scheme and structure uniform grid system are employed to discretize the main governing equation as shown in Fig. 1(b). The solutions are considered to be converged when the normalized residual values reach (10^{-5}) for all variables.

2.5. Code validations and grid testing

In order to assess the accuracy of the numerical procedure, the domain for a 2D channel with length and height (100×12.5) mm^2 has been tested. To evaluate the number of elements required, four different meshes have been tested. The grid independence test is carried out in the analysis by adopting different grid distributions of 24,000, 34,000, 48,000 and 88,000. The grid independence test indicated that the grid systems of 48,000 ensure a satisfactory solution. It is found that after 48,000 cells, further increase in cells give less than 2% variation in average Nusselt number value which is taken as criterion for grid independence. To validate the numerical code used in the present study, Fig. 2 shows the average corrugated plate temperature for air flow through two opposite corrugated plats is calculated and compared with numerical and experimental study of Naphon [6].

3. Results and discussion

The numerical study presented in this work considered a nanofluid compound of four different nanoparticles, different volume fractions immersed in the different base fluid.

3.1. The effect of different nanoparticles types

In this section, four different types of nanoparticles: Al_2O_3,CuO, SiO_2 and ZnO with water as a base fluid are used. The nanoparticle concentration used in this case is 4% and the nanoparticle diameter is 20 nm.In order to see the effect of different nanofluids on the heat transfer enhancement all other parameters of the system of heat transfer should be fixed. The Nusselt number for different nanofluids at wavy angle$=60^\circ$, wavy height $=2.5$ mm, channel height $=17.5$ mm and different Reynolds numbers is shown in Fig. 3(a). It can be seen that the Nusselt number increases with the increase of Reynolds number for all cases. It is observed that all four nanofluids possess higher Nusselt number compared to pure water. These results also indicate that all the four types of nanofluids are comparatively richer in heat transfer rate than the pure water. But in case of comparison the four types of nanofluids, it is clear that the nanofluid with SiO_2 has the highest value, followed by Al_2O_3, ZnO and finally CuO. At the inlet, the heat transfer rate is directly related to thermophysical properties of the fluids, thus having lower thermal conductivity places SiO_2 higher other nanofluds and water. The effect of various nanofluids on the pressure drop is shown in Fig. 3(b). The nanoparticle concentration considered is 4% for different Reynolds numbers. It can be seen that the SiO_2 nanofluids has the highest pressure drop, followed by Al_2O_3, ZnO, CuO and finally water. In order to better explain this situation, it must be noted that lower mean

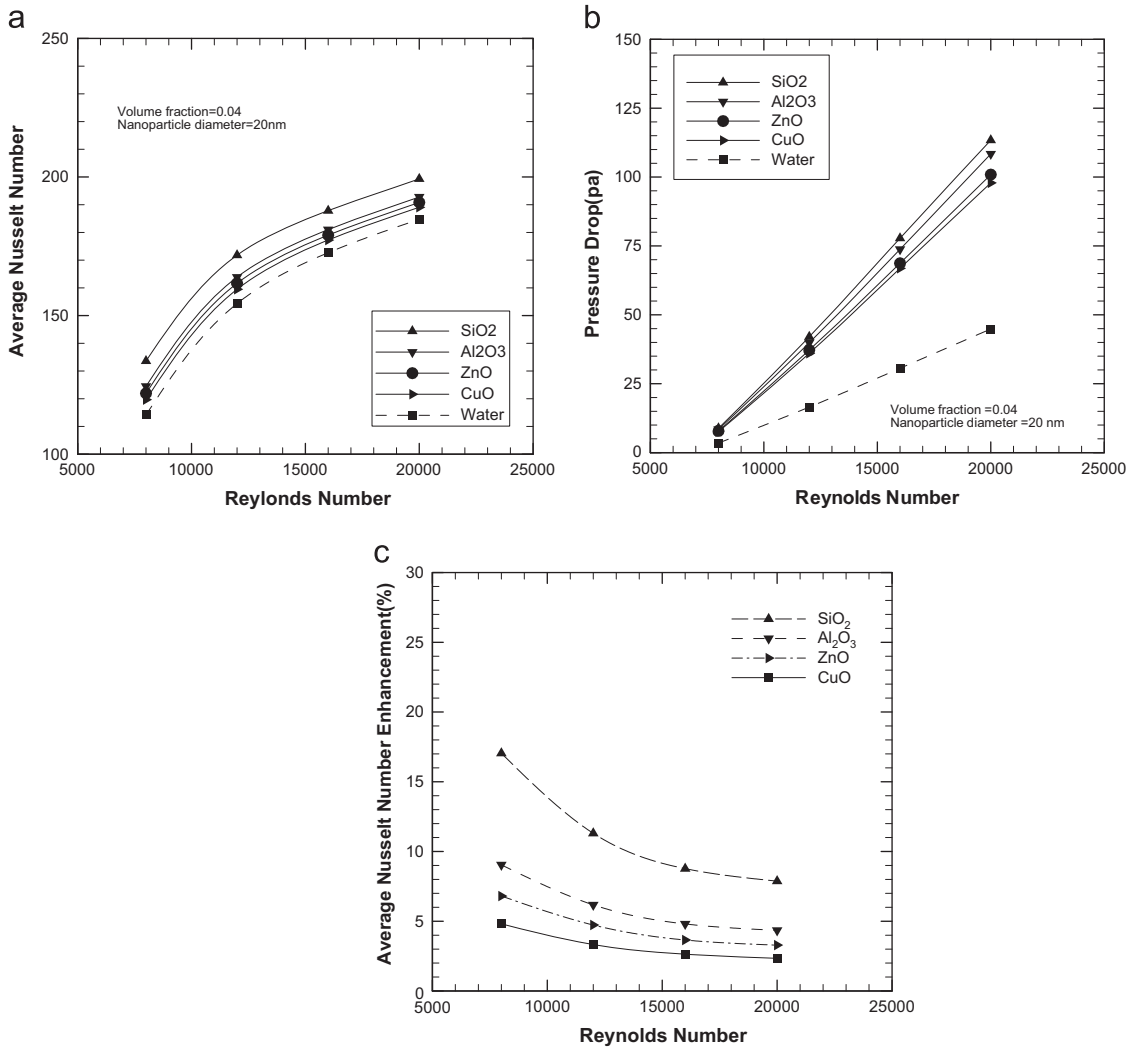

Fig. 3. The effect of different nanofluids types under Reynolds number range on the: (a) average Nusselt number, (b) pressure drop, and (c) average Nusselt number enhancement.

velocity gives lower velocity gradient among the fluids and channel walls, which in turn reduces the wall shear stress. Fig. 3(c) illustrates the average Nusselt Number Enhancement versus Reynolds number for different nanoparticles types. It can be seen that the heat transfer enhancement decreases as Reynolds number increases for all type of nanofluids. It is also shown that the SiO_2 yielded better heat transfer enhancement than other types of nanofluids. It is observed that addition of 4% nanoparticles (SiO_2, Al_2O_3, ZnO, CuO) to the base fluid can enhance the heat exchange by 14%, 7.5%,5.7% and 4%, respectively, with respect to those corresponding to the case $d_p = 20$ nm and Re = 1000.

3.2. The effect of different nanoparticles volume fractions

The volume fraction of nanoparticles is actually referred to the volume of nanoparticles constituent divided by the volume of the all constituents of the mixture prior to mixing. In other words, possessing more nanoparticles within base fluid leads to get nanofluid with greater amount of volume fraction (concentration) [25]. Fig. 4(a) illustrates the effects of nanoparticle and volume fraction on Nusselt number. It demonstrates that adding low volume fraction of nanoparticle (0–0.04) with particle diameter of 20 nm for SiO_2 to the base fluid leads to significant increase in Nusselt number. This is indication that the presence causing of nanoparticles clearly enhance heat absorption of the coolant causing its temperature to increase. In general, these enhancements are due to higher thermal conductivity of nanoparticles and the role of Brownian motion of nanoparticles on enhancement of thermal conductivity which is due to larger surface area of nanoparticles for molecular collisions. The higher mass concentrations of nanoparticles compared to the base fluid molecules have higher momentum, this momentum carry and transfer thermal energy more efficiently at greater distance inside the base fluid before releasing the thermal energy in colder regions of the fluid (small packets of energy) [26]. It can

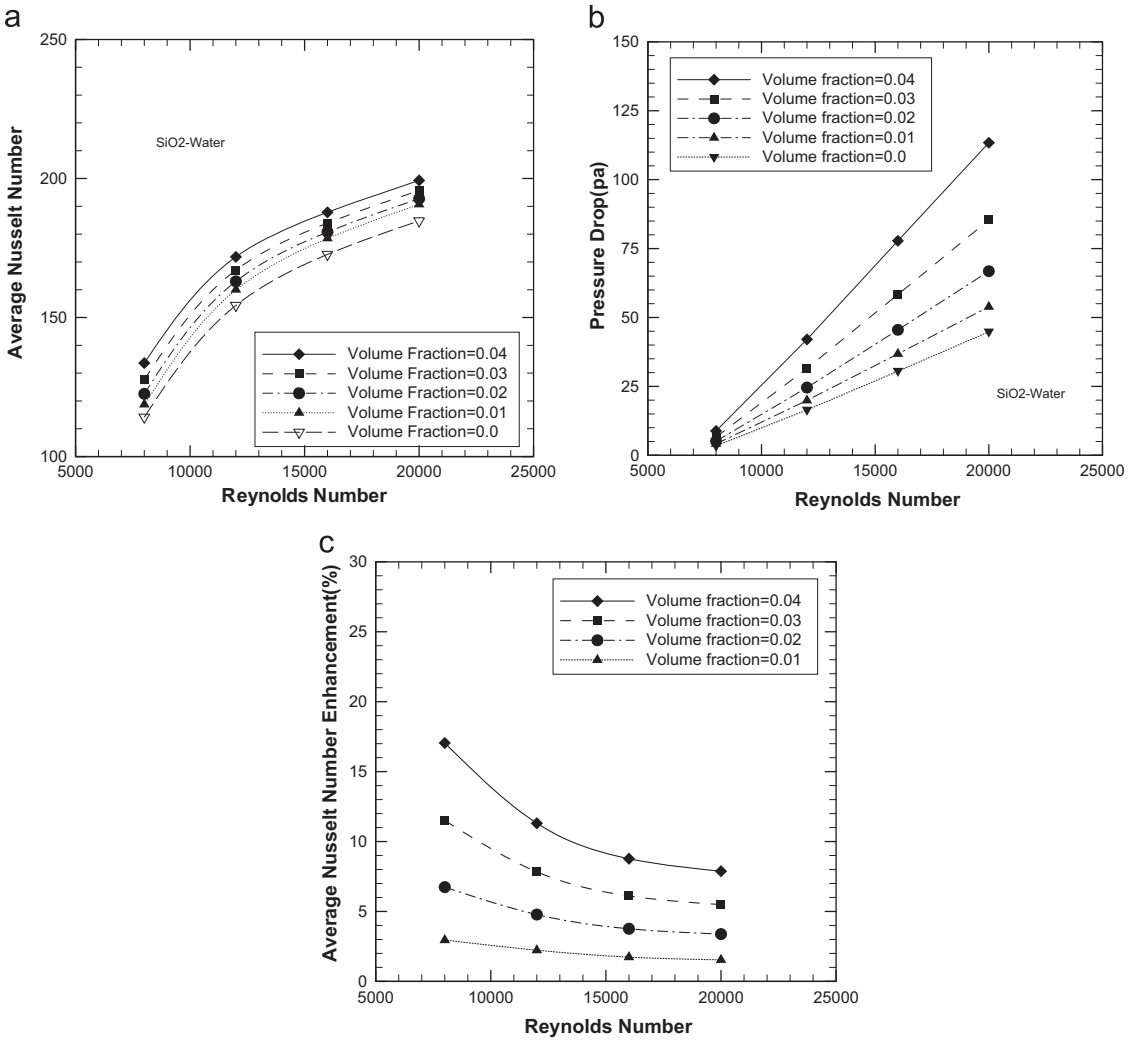

Fig. 4. The effect of different volume fraction under the Reynolds number range on the: (a) average Nusselt Number, (b) pressure drop, (c) average Nusselt number enhancement.

be seen that the Nusselt number increases with increased value of volume fraction. As shown in the Fig. 4(b) the results show that the pressure drop of the SiO_2–water increases with the increase of Reynolds number and nanoparticle concentration. One notices that the pressure drop is dependent on density and viscosity of the fluids. With an increase in the particle volumetric concentration in the nanofluids the density and viscosity increase and hence they cause an increased pressure drop [12]. Fig. 4(c) shows that the increasing volume fraction of nanoparticles, which is responsible for large heat transfer performance leads to higher pressure drop. It should be noted that the enhancement in heat transfer increases with the increase of volume fraction of nanoparticles at the same value of Reynolds number. Appreciable increase more than 12% in the average Nusselt number enhancement for the nanofluids with 4% of SiO_2 nanoparticle at low Reynolds number compared to the case of pure water is obtained. As it is expected for a low particle concentration the enhancement is very low ($\sim$2.5%).

3.3. *The effect of different base fluids*

The effects of different types of base fluids on the Nusselt number versus the Reynolds number are shown in Fig. 5(a). It can be seen that the SiO_2–glycerin has the highest value of Nusselt number followed by SiO_2–ethylene-glycol while the SiO_2–water has the lowest value of Nusselt number. It is observed that the Nusselt number increases when the Reynolds number increases for different base fluids. It is seen, however, the presence of SiO_2 nanoparticle in glycerin could greatly enhance the heat transfer compared with other types of base fluid studied. This is because glycerin has the highest dynamic viscosity in nature compared to other base fluids. The influence of Reynolds number on the pressure drop of SiO_2 nanoparticle of different base fluids is shown in Fig. 5(b). The nanoparticle concentration considered in this case is 4% and

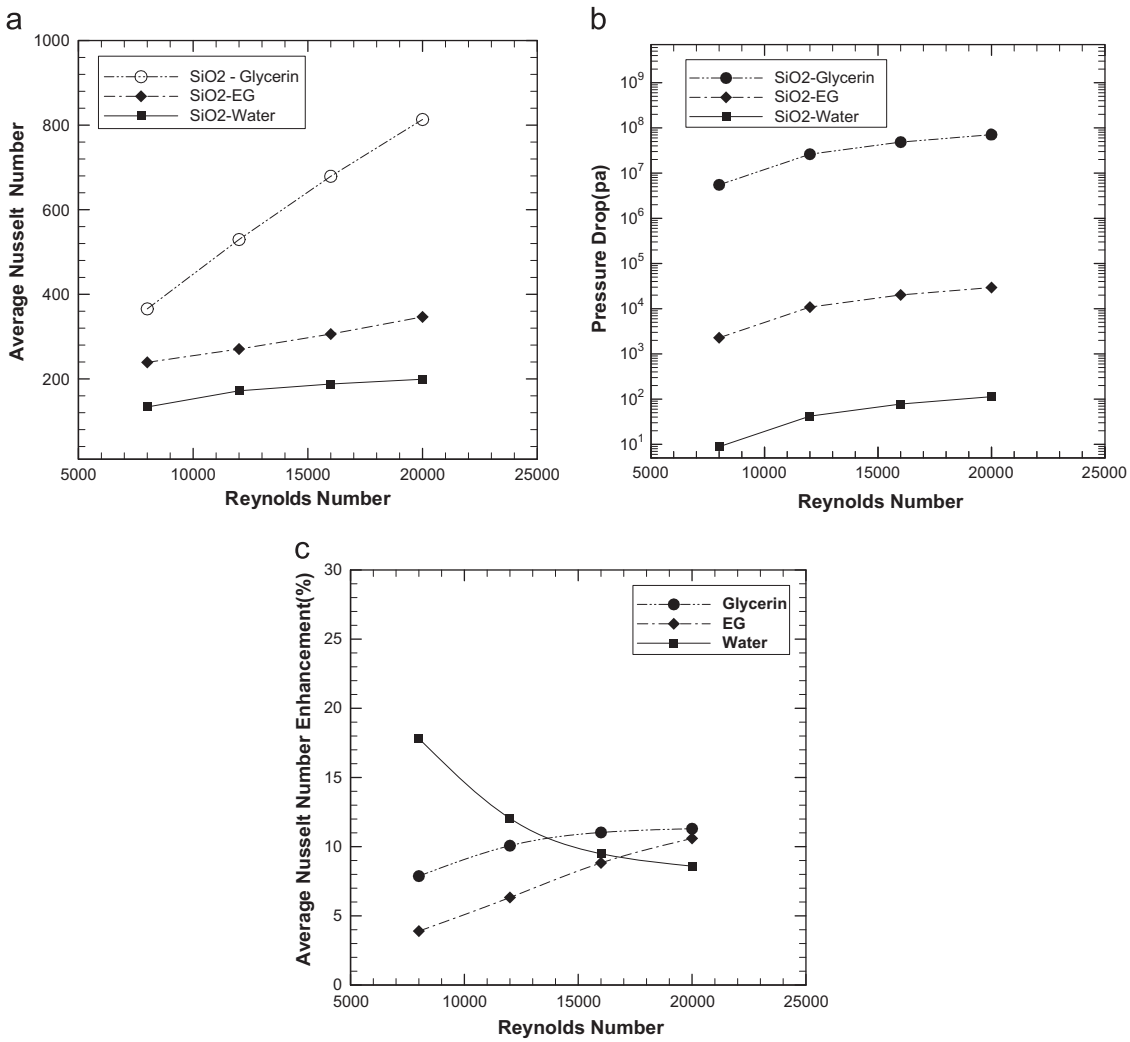

Fig. 5. The effect of different base fluids under the Reynolds number range on the: (a) average Nusselt number, (b) pressure drop, and (c) average Nusselt number enhancement.

Table 3
The characteristics of nanofluids and different base fluids at $d_p = 20$ nm and $\varnothing = 4\%$.

Property	EG	EG + SiO_2	Glycerin	Glycerin + SiO_2	Water	Water + SiO_2
Density, ρ (kg/m^3)	1114.4	1157.824	1259.9	1297.504	996.5	1044.64
Specific heat,C_p (J/kg K)	2415	2288.0722	2427	2312.92251	4181	3891.5529
Thermal conductivity, k (W/m K), Static		0.2706835		0.305835886		0.63263843
Thermal conductivity, k (W/m K), Brownian		0.0054439		0.00618527		0.00842772
Thermal conductivity, k (W/m K), effective	0.252	0.2761274	0.286	0.312021156	0.6103	0.64106615
Dynamic viscosity, μ (Ns/m^2)	0.0157	0.0277144	0.799	1.440379518	0.00100	0.00163700

nanoparticles diameter is 20 nm. The SiO_2–glycerin has higher pressure drop followed by SiO_2–ethylene-glycol and SiO_2–water. It can be seen that the pressure drop increase with the increase Reynolds number. It is observed that the increased the velocity along the channels with the increase in Reynolds number results in higher shear stress, which results in higher pressure drop. The effects of different types of base fluids on the average Nusselt number enhancement versus Reynolds number are shown in Fig. 5(c). It is demonstrated that significant enhancement in heat transfer may occur due to thermophysical properties for the fluids with high viscosity and low heat capacity, subjected to high Reynolds number flow. The contrary trends observed in average Nusselt number enhancement for the water based nanofluids could be due to the higher thermal conductivity and lower viscosity, which should have important effects on heat transfer enhancement. Results show that base fluids having a lower dynamic viscosity, such as water, provide better heat transfer performance

under low Reynolds number. A substrate having a higher thermal conductivity yields better heat transfer enhancement. Whereas the Glycerin-based nanofluid shows greater heat transfer enhancement among all base fluids under high Reynolds number. Table 3 shows that, for a given particle volume fraction, the EG+SiO_2 has a lower thermal conductivity and heat capacity than Glycerin+SiO_2 and water+SiO_2, while the Glycerin+SiO_2 has higher dynamic viscosity than that of EG+SiO_2 and water+SiO_2. It can be seen that the density and thermal conductivity for the nanofluids increased and specific heat decreased slightly in compare to base fluid. Viscosity increases more markedly, which is unfavorable in heat transfer.

4. Conclusions

The turbulent convective of four nanofluids types Al_2O_3,CuO, SiO_2 and ZnO flowing in a V-shaped corrugated channel under constant heat flux boundary condition have been numerically investigated. The effects of nanoparticle types, nanoparticle concentration (∅), and type of base fluid on the thermal and hydraulic behavior of V-shaped wavy lower plate have been examined. The potential of developing combined V-shaped wavy lower plate with nanofluid as cooling using various particle volume fractions and base fluids in enhancing the heat transfer, the following findings can be drawn:

- The results show that the SiO_2 gives the highest Nusselt number and pressure drop followed by Al_2O_3, ZnO and CuO respectively while the pure water gives the lowest Nusselt number and pressure drop.
- The Nusselt number and pressure drop increased by increasing the nanoparticle volume fractions.
- Results clearly showed that the presence of nanoparticles produced a significant increase of the heat transfer with respect to that of the base liquid. Heat transfer enhancement was increasing with the nanoparticle volume fractions and can enhance the heat exchange by 14%, 7.5%,5.7% and 4%, respectively, with addition of 4% nanoparticles (SiO_2, Al_2O_3, ZnO, CuO) to the base fluid.
- The SiO_2–glycerin has the highest value of Nusselt number, while the SiO_2–water has the lowest value of Nusselt number. The water based nanofluids, provide better heat transfer performance under low Reynolds number. While the Glycerin-based nanofluid shows greater heat transfer enhancement among all base fluids under high Reynolds number.

References

[1] Islamoglu Y, Parmaksizoglu C. The effect of channel height on the enhanced heat transfer characteristics in a corrugated heat exchanger channel. Appl Therm Eng 2003;23:979–87.
[2] Islamoglu Y, Parmaksizoglu C. Numerical investigation of convective heat transfer and pressure drop in a corrugated heat exchanger channel. Appl Therm Eng 2004;24:141–7.
[3] Naphon P. Laminar convective heat transfer and pressure drop in the corrugated channels. Int Commun Heat Mass Transf 2007;34:62–71.
[4] Naphon P. Heat transfer characteristics and pressure drop in channel with V corrugated upper and lower plates. Energy Convers Manag 2007;48: 1516–24.
[5] Wang C-C, Chen C-K. Forced convection in a wavy-wall channel. Int J Heat Mass Transf 2002;45:2587–95.
[6] Naphon P. Effect of corrugated plates in an in-phase arrangement on the heat transfer and flow developments. Int J Heat Mass Transf 2008;51: 3963–71.
[7] Naphon P. Effect of wavy plate geometry configurations on the temperature and flow distributions. Int Commun Heat Mass Transf 2009;36:942–6.
[8] Naphon P, Kornkumjayrit K. Numerical analysis on the fluid flow and heat transfer in the channel with V-shaped wavy lower plate. Intl Commun Heat Mass Transf 2008;35:839–43.
[9] Lee G-J, Kim CK, Lee MK, Rhee CK, Kim S, Kim C. Thermal conductivity enhancement of ZnO nanofluid using a one-step physical method. Thermochim Acta 2012;542:24–7.
[10] Das SK, Putra N, Thiesen P, Roetzel W. Temperature dependence of thermal conductivity enhancement for nanofluids. J Heat Transf 2003;125:567–74.
[11] Vajjha RS, Das DK. Experimental determination of thermal conductivity of three nanofluids and development of new correlations. Int J Heat Mass Transf 2009;52:4675–82.
[12] Vajjha RS, Das DK, Kulkarni DP. Development of new correlations for convective heat transfer and friction factor in turbulent regime for nanofluids. Int J Heat Mass Transf 2010;53:4607–18.
[13] Koo J, Kleinstreuer C. Viscous dissipation effects in microtubes and microchannels. Int J Heat Mass Transf 2004;47:3159–69.
[14] Corcione M. Heat transfer features of buoyancy-driven nanofluids inside rectangular enclosures differentially heated at the sidewalls. Int J Therm Sci 2010;49:1536–46.
[15] Heidary H, Kermani M. Effect of nano-particles on forced convection in sinusoidal-wall channel. Int Commun Heat Mass Transf 2010;37:1520–7.
[16] Ahmed M, Shuaib N, Yusoff M. Numerical investigations on the heat transfer enhancement in a wavy channel using nanofluid. Int J Heat Mass Transf 2012;55:5891–8.
[17] Ahmed M, Shuaib N, Yusoff M, Al-Falahi A. Numerical investigations of flow and heat transfer enhancement in a corrugated channel using nanofluid. Int Commun Heat Mass Transf 2011;38:1368–75.
[18] Xuan Y, Li Q. Heat transfer enhancement of nanofluids. Int J Heat Fluid Flow 2000;21:58–64.
[19] Xuan Y, Roetzel W. Conceptions for heat transfer correlation of nanofluids. Int J Heat Mass Transf 2000;43:3701–7.
[20] Buongiorno J. Convective transport in nanofluids. J Heat Transf 2006;128:240–50.
[21] Bianco V, Chiacchio F, Manca O, Nardini S. Numerical investigation of nanofluids forced convection in circular tubes. Appl Therm Eng 2009;29: 3632–42.
[22] Versteeg HK, Malalasekera W. An Introduction to Computational Fluid Dynamics. Longman Group; 1995.
[23] Launder BE, Spalding D. The numerical computation of turbulent flows. Comput Methods in Appl Mech Eng 1974;3:269–89.
[24] Incropera FP, Dewitt DP. In: Fundamentals of Heat and Mass Transfer. 5th edition, New York: John Wiley and Sons; 2002.
[25] Manca O, Jaluria Y, Poulikakos D. Heat transfer in nanofluids. Adv Mech Eng 2010:2010.
[26] Seyf HR, Feizbakhshi M. Computational analysis of nanofluid effects on convective heat transfer enhancement of micro-pin-fin heat sinks. Int J Therm Sci 2012;58:168–79.